Chapter 39
Mitigation of Ionospheric Delay in GPS/BDS Single Frequency PPP: Assessment and Application

Zishen Li, Lei Fan, Yunbin Yuan, Sandra Verhagen, Peter de Bakker, Hong Yuan and Shiming Zhong

Abstract Single-frequency (SF) Precise Point Positioning (PPP) is a promising technique for real-time positioning and navigation at sub-meter (about 0.5 m) accuracy level because of its convenience and low cost. With satellite orbit and clock error being greatly mitigated by the precise products from the International GNSS Service (IGS), ionospheric delay becomes the bottleneck of SF PPP users. There are five commonly used approaches to mitigate ionospheric delay in SF PPP: (1) broadcast ionospheric model in Global Navigation Satellite System (GNSS) navigation message; (2) global ionospheric map released by the IGS; (3) local ionospheric model generated using GNSS data from surrounding reference stations; (4) satellite based ionospheric model; (5) the parameter estimation method. Those approaches are briefly reviewed in our contribution and the performances of some classical ionospheric approaches for SF PPP are validated and compared using GPS data from two networks in China and the Netherlands respectively. Validation results show that a set of reference stations is critical for SF PPP with sub-meter positioning accuracy, especially in China. It is better to model the ionospheric delay in a satellite by satellite mode rather than an integral mode under the assumption of a thin-layer ionosphere. Comparing to GIM, the suggested approach, satellite based ionospheric model (SIM), can improve the horizontal positioning accuracy of SF PPP from 0.40 to 0.10 m in China and from 0.20 to 0.05 m in the Netherlands, while it can improve the vertical accuracy from 0.70 to 0.15 m (China) and from 0.20 to 0.10 m (the Netherlands). Furthermore, the recommended ionospheric model has been applied to GPS/BDS data for SF

Z. Li (✉) · H. Yuan
Academy of Opto-Electronics, Chinese Academy of Sciences, Beijing 100094, China
e-mail: lizishen@aoe.ac.cn

Z. Li · L. Fan · Y. Yuan · S. Zhong
State Key Laboratory of Geodesy and Earth's Dynamics, Institute of Geodesy
and Geophysics, Chinese Academy of Sciences, Wuhan 430074, China

S. Verhagen · P. de Bakker
Delft University of Technology, Delft 2600 GA, The Netherlands

PPP as well. The experiment in Beijing shows that the positioning of about 0.5 m accuracy can be achieved by single epoch SF PPP based on a reference network of about 40 km inter-station distance. The accuracy of SF PPP based on an accumulation of 10–15 min of observations in dynamic mode is about 0.04 m (horizontal) and 0.04–0.08 m (vertical) using only GPS data, while it is about 0.03 m (horizontal) and 0.03–0.06 m (vertical) by combining GPS and BDS data.

Keywords Ionospheric delay mitigation · SIM · Single frequency precise point positioning · GPS · BDS

39.1 Introduction

There is a tremendous demand for real-time positioning with sub-meter (about 0.5 m) accuracy in the modern urban management, such as traffic guidance, urban planning, emergency rescue etc. PPP is a very efficient and convenient GNSS (Global Navigation Satellite System) positioning approach since it only relies on a GNSS receiver and correction data from a reference network. The PPP technique, which was firstly introduced by Zumberge et al. [44], can achieve decimeter to centimeter level positioning accuracy by applying various corrections, such as satellite orbit, satellite clock, ionospheric delay, and tropospheric delay [3, 20, 21]. In order to mitigate the ionospheric delay, dual-frequency signals are usually required in the traditional PPP technique. However, a dual-frequency receiver is too expensive for many applications and the high cost is currently one of the major barriers for the PPP technique in many common applications. Actually, reasonable accuracy at a low cost is preferred by many potential PPP users, e.g. a positioning with about 0.5 m accuracy is usually sufficient for the lane identification [37]. Therefore, PPP technique with single frequency receiver can be a perfect solution balancing the positioning accuracy and acceptable cost.

Ionosphere delay is one of the major challenges of single frequency (SF) PPP, because it cannot be eliminated without dual-frequency signals. SF PPP can be expected to perform well only when the ionospheric delay is accurately mitigated. However, the variations and characteristics of ionospheric delay are usually difficult to be modeled. Numerous approaches for mitigating the ionospheric delay of SF PPP have been studied in previous literature [1, 4, 23, 28, 33, 34]. Generally, these approaches can be divided into five levels based on the accuracy and implement method.

(1) Broadcast Ionospheric Model (BIM): this model is distributed along satellite ephemeris in the navigation message, such as GPS Klobuchar model [17, 18], BDS Klobuchar-like model [2, 38]. Due to the simplicity of model and

limitation of updating interval, however, BIM can only achieve the correction of about 0.5–1.2 m and 2.0–2.6 m on the zenith direction at low and high ionospheric activities respectively [8, 38, 40]. Therefore, BIM is generally not sufficiently accurate for SF PPP to achieve sub-meter level positioning.

(2) Global Ionospheric Map (GIM): it is one of the most popular ionospheric products for SF PPP. The ionospheric Total Electron Content (TEC) values are represented on a global scale grid and updates every two hours [31]. Currently, the IGS released GIM is a combined products from four ionospheric associate analysis centres [15]. The nominal accuracy of GIM is about 0.30–0.80 m in the zenith direction on average, but it is even lower in areas with fewer contributing GNSS stations [29, 46].

(3) Local Ionospheric Map (LIM): it characterizes vertical ionospheric delay over a small region with dual-frequency GNSS data from local reference stations. In contrast to GIM, the local real-time GNSS data contributes to the LIM estimation and the ionospheric delay provided by LIM is usually of a better accuracy. How to select a mathematic function to represent the variation in local ionospheric delay is one of the most critical issues for LIM. Many functions have been studied, including polynomial function [6], triangle series function [12, 39] (adjusted) low order spherical harmonic function [32, 46], and spherical cap harmonic function [26]. However, the LIM is generally established under the assumption of ionospheric thin-layer, a so-called mapping function is required for converting ionospheric delay from the line-of-sight (LOS) to vertical direction. The lower the satellite elevation, the larger the error resulting from the mapping function [47].

(4) Satellite based Ionospheric Map (SIM): SIM is a new regional ionospheric delay modeling method aiming to provide high accuracy ionospheric delay. In SIM, the LOS ionospheric delay at the rover station is directly derived from the corresponding observation of surrounding reference stations without a thin-layer assumption and mapping function. It has been used to reduce dual-frequency PPP convergence time and mitigate the ionospheric delay in SF PPP [11, 28, 41, 42, 45]. This method is more straightforward; the difference of satellite elevations between different stations is not considered any more. Therefore, this approach is more suitable for regional ionosphere modeling.

(5) Parameterized Ionospheric Model (PIM): Different from the aforementioned four ionospheric modeling methods, the LOS ionospheric delay in PIM is modeled by a number of unknown parameters and estimated simultaneously with positioning, e.g. the vertical delay and two gradient components [24, 34], a time variant parameter for each satellite (GRAPHIC, Group And Phase Ionospheric Correction) [5] etc. However, prior ionosphere information is still essential for this method to improve the parameter estimation. Otherwise, the long convergence time will become unacceptable for real-time or near real-time users.

According to the above analysis, a precise ionospheric model is very essential for the sub-meter level SF PPP. In view of this, we will focus on the mitigation method of ionospheric delays for a SF PPP user, including some assessments and

applications. The following parts of this paper are organized as follows: Sect. 39.2 briefly reviews some commonly used approaches applicable for SF PPP user; Sect. 39.3 validates their performances using real GPS data from two networks in both China and the Netherlands, and provides some useful suggestions on ionospheric delay correction for SF PPP users; Sect. 39.4 attempts to apply the recommend approach identified in Sect. 39.3 in SF PPP using a preliminary GPS/BDS dataset; finally, Sect. 39.5 summarizes some major findings in this paper and future work.

## 39.2 Review of Some Classical Ionospheric Models for SF PPP User

The purpose of this contribution is to find a preferred ionospheric model for local SF PPP by comparing the performance of commonly used approaches. Before this comparison, some classical ionospheric models for SF PPP users is briefly reviewed in this section, including global ionospheric map, local ionospheric model and satellite based ionospheric model.

39.2.1 Global Ionospheric Map-GIM

The GIM defined in the IONosphere map EXchange format (IONEX) is a public product released by IGS and generated by combining the daily GIMs from four ionospheric associate analysis centres (IAACs), including Center for Orbit Determination in Europe (CODE; University of Berne, Switzerland), Jet Propulsion Laboratory (JPL; Pasadena, California, USA), European Space Operations Center of European Space Agency (ESOC; Darmstadt, Germany), and Technical University of Catalonia/gAGE (UPC; Barcelona, Spain) [14]. The GIM from each IAAC is evaluated by comparing the differences of TEC from itself and real GNSS data and a weight is calculated for the final combination based on these differences [16].

Different strategies have been adopted for ionospheric TEC modeling by those IAACs. The global ionospheric vertical TEC (vTEC) over a single day is represented by a series of spherical harmonic expansions up to degree and order of 15 with a 2-h temporal resolution by CODE and ESOC, whereas it is represented by a linear composition of bi-cubic splines with 1,280 spherical triangles and 15 min resolution by JPL [9, 10, 19, 32]. The current ionospheric TEC models used by CODE, JPL, and ESOC are all based on the ionospheric thin-layer assumption, and a mapping function is necessary for converting the ionospheric TEC from LOS to vertical direction. Different from those approaches used by CODE, JPL and ESOC, UPC GIM is produced by interpolating the vTEC over each ionospheric IPP. The vTEC is computed by means of a two-layer (450 and 1130 km) tomographic approach over each individual station [13, 30]. The LOS ionospheric TEC is

Fig. 39.1 Interpolation of rover LOS ionospheric delay using the surrounding 4 TEC values
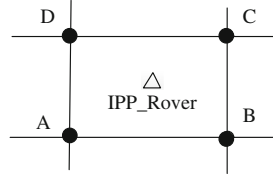
extracted from dual-frequency data by the geometry free combination of phase-smoothed code. The differential code biases (DCB) in satellites and contributing receivers is estimated simultaneously with the global ionospheric TEC modeling.

With GIM, the TEC values are defined on a 5° (longitude) × 2.5° (latitude) grid with a 2-h temporal resolution. In order to apply GIM to SF PPP, the vTEC at one satellite IPP for the rover needs to be firstly interpolated between two consecutive maps and then mapped to the LOS ionospheric delay [31]. The interpolation and mapping method is shown by Fig. 39.1 and Eq. (39.1). The solid dots in Fig. 39.1 are four surrounding grid points defined in GIM and the triangle is the location of rover ionospheric IPP.

$$
\begin{cases}
I_{r,t} = VTEC_{r,t} \cdot mf(z) \cdot A \\
VTEC_{r,t} = \dfrac{t_2 - t}{t_2 - t_1} VTEC_{r,t_1} + \dfrac{t - t_1}{t_2 - t_1} VTEC_{r,t_2} \\
VTEC_{r,t_i} = (1 - p) \cdot (1 - q) \cdot VTEC_{A,t_i} + p \cdot (1 - q) \cdot VTEC_{B,t_i} \\
\qquad\qquad + p \cdot q \cdot VTEC_{C,t_i} + q \cdot (1 - p) \cdot VTEC_{D,t_i} \quad (i = 1, 2) \\
p = \dfrac{\varphi_r - \varphi_A}{d\varphi}, q = \dfrac{\lambda_r - \lambda_A}{d\lambda}
\end{cases}
$$

$$(39.1)$$

where $I_{r,t}$ is the predicted ionospheric delay of one satellite at t for rover r; $VTEC_{r,t}$ is the vTEC for the rover interpolated from the GIM; $mf(z)$ is the mapping function defined as $mf(z) = (1 - \sin^2 z)^{-2}$, where z is the satellite's zenith distance at corresponding IPP; A is a constant value used to convert TEC unit to length unit, defined as $A = 40.28 \cdot 10^{16} \cdot f^{-2}$; f is the frequency on which the code and phase are used for SF PPP; t_1 and t_2 are the nearest two times at which the map is selected for interpolation, assuming $t_2 \geq t \geq t_1$; $VTEC_{r,t_1}$ and $VTEC_{r,t_2}$ are the corresponding vTEC obtained from the ionospheric map at t_1 and t_2, respectively; $VTEC_{A,t_i}$, $VTEC_{B,t_i}$, $VTEC_{C,t_i}$ and $VTEC_{D,t_i}$ are the ionospheric vTEC at grid point A, B, C and D respectively; φ_r and λ_r are the geographic latitude and solar longitude of ionospheric IPP at rover; λ_A and φ_A are the geographic latitude and solar longitude of grid point A; $d\varphi$ and $d\lambda$ are the interval of latitude and longitude in GIM, $d\varphi = 2.5°$ and $d\lambda = 5°$ for IGS released GIM; The ionospheric delay for each satellite can be individually predicted using Eq. (39.1).

The final and predicted GIMs are all released by IGS. The latency of final product is about 2 weeks and thus cannot be used in real-time or near-real-time

application. The predicted product is released 1–4 days ahead and is feasible for real-time SF PPP. With the IGS GIM product, the users are able to acquire precise ionospheric delay without setting up new reference stations for monitoring the ionosphere. In our experiment, GIM refers the IGS predicted product.

39.2.2 Local Ionospheric Model-LIM

A small-scale network equipped with dual-frequency receivers is also capable to provide precise ionospheric delay. Those dual-frequency receivers are also named reference stations. LIM is established using the LOS ionospheric TEC extracted from the raw data of reference stations with DCB correction. Generally, the variation in ionospheric vTEC over a small area (e.g. 20–80 km) is very smooth and easy to be represented by the polynomial. The mapping function is also necessary in LIM. The coefficients of polynomial ionospheric model are broadcasted to the rover along with their variances. After receiving the coefficients and its RMS of polynomial based ionospheric model, the rovers can calculate their own ionospheric delay and variances for each satellite. The polynomial ionospheric model is generally described as [6]:

$$I_{r,t} = A \cdot mf(z) \cdot \sum_{n=0}^{N} \sum_{m=0}^{M} E_{nm,t} \left(\beta_{r,t} - \beta_0 \right)^n \left(s_{r,t} - s_0 \right)^m \tag{39.2}$$

where, $I_{r,t}$ is the predicted ionospheric delay of one satellite at epoch t for rover r; $\beta_{r,t}$, $s_{r,t}$ are the latitude and longitude of rover ionospheric IPP, respectively; β_0 and s_0 are the latitude and longitude of the geometric center of polynomial model; N and M are the maximum orders of the polynomial model in terms of latitude and longitude respectively and E_{nm} represents the unknown coefficients of polynomial model estimated using the data from reference network. In our experiment, a second order polynomial model is adopted, i.e. $N = M = 2$.

Based on LIM, the real-time data from reference stations is contributed to local ionospheric modeling; thus, the accuracy of ionospheric delay from LIM is usually higher than that of GIM. In order to improve the temporal resolution of ionospheric modeling, the LIM is updated every epoch in our experiment, but the latency of data transmission is not considered.

39.2.3 Satellite based Ionospheric Model-SIM

Both GIM and LIM assume that the LOS ionospheric TEC is concentrated on a shell of infinitesimal thickness and a mapping function is commonly used to convert the LOS ionospheric TEC to vTEC. The mapping function is defined as an approximate trigonometric function, e.g. single-layer mapping function (SLM), or

modified SLM etc. [22, 27, 32]. However, the variation of LOS ionospheric TEC is very complex and the distribution of ionospheric density cannot be completely described by vTEC plus mapping function. Moreover, the mapping function cannot reflect the azimuth-dependent variations in ionospheric TEC. Previous study demonstrated that the modeling error resulted by the ionospheric thin-layer assumption and mapping function is about 0.05–0.20 m at different levels of ionospheric activities [7, 46, 47]. Thus, the modeling error cannot be acceptable for the ionospheric delay correction of 0.10–0.20 m accuracy level.

In order to reduce the modeling error, a satellite based ionospheric model (SIM) is developed using regional reference stations. It represents the LOS ionospheric delay on a satellite basis rather than ionospheric vTEC with mapping function. The SIM has been used by Geng et al. [11] and Zhang et al. [41] for estimating the ionospheric delay with a relatively high precision to reduce the convergence time of dual-frequency PPP. Different modeling/interpolation methods can be used in SIM, e.g. inter-stations weighted average and Kriging interpolation [28, 42, 43]. In this contribution, the ionospheric delay for the rover is interpolated according to the relative geographical locations of reference stations and rover, shown by Eq. (39.3).

$$
\begin{cases}
I_{r,t}^s = \sum_{i=1}^{N} P_i^s I_{i,t}^s \\
P_i^s = \left(D_{i,r} \cdot \sum_{m=1}^{N} D_{m,r}^{-1} \right)
\end{cases}
\tag{39.3}
$$

where $I_{r,t}^s$ is the LOS ionospheric delay correction of satellite s to rover r at time t; N is the number of surrounding reference stations; $I_{i,t}^s$ is the LOS ionospheric delay of satellite s to station i at epoch t; $D_{i,r}$ is the spherical distance between rover and station i; $D_{m,r}$ is the spherical distance between rover and station m.

It can be found that the SIM is based on the approximation that the elevations of one satellite at those reference and rover stations are considered the same. Thus, although SIM can avoid the modelling error caused by the mapping function, a new modelling error resulting from this approximation is introduced. Generally, the approximation is very reasonable for small-scale network, but the error caused by the approximation will become larger with the increasing of inter-station distance. So, SIM is very suitable to predict precise ionospheric delays for a rover from a small-scale network.

39.3 Assessment and Comparison of Different Ionospheric Delay Mitigation Models in SF PPP

The accuracy of ionospheric delay correction is the major barrier hindering SF PPP centimeter accuracy positioning, currently only achievable using a dual-frequency PPP technique [21, 23]. In this section, the aforementioned approaches are applied

(Latitude: 38.5⁰N-40.0⁰N)   (Latitude: 50.5⁰N-52.5⁰N)
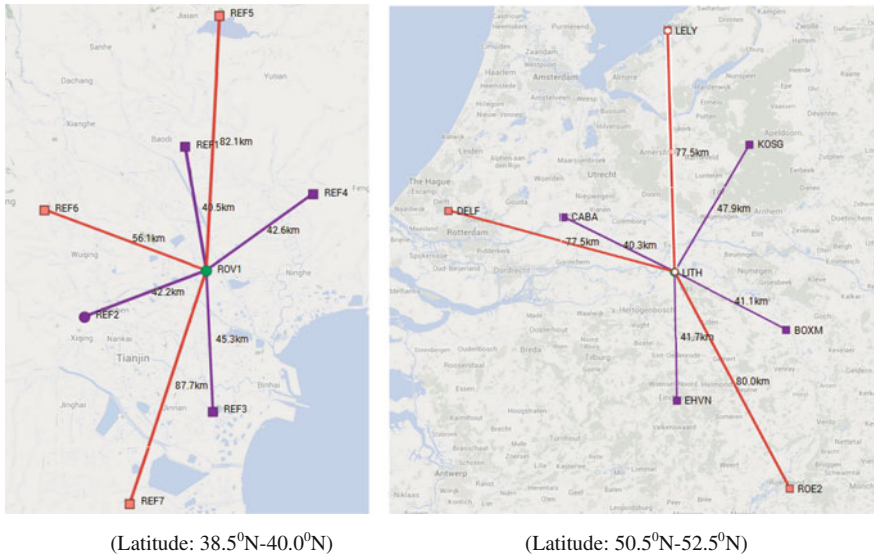
Fig. 39.2 Distribution of networks in China (*left*) and the Netherlands (*right*) in the experiment

to SF PPP data processing and their performances are assessed and compared. Some useful suggestions about ionospheric delay mitigation in SF PPP are summarized from their performance comparison between different approaches.

39.3.1 Description of GPS Data

Two GPS networks in China and the Netherlands are selected for this experiment respectively. Each network involves eight stations, the station in the center is considered as the rover and the other surrounding stations are used as reference stations. The locations and the distance between the rover and the reference stations are marked in Fig. 39.2. Both networks are located in middle latitudes (38°N–53°N), and the global ionospheric activities are at a medium level during the experimental period.

All the reference stations are divided into two groups according to the distance to the rover station. The distances in different groups are about 40 and 80 km respectively, and they are very typical for GNSS application in urban area. Using two sub-networks can reflect the variations of ionospheric modeling in different inter-station distances scenarios.

The type of antenna and receiver of selected stations at each station are listed in Table 39.1. The network in China is equipped with exactly the same antennas and receivers, whereas the network in the Netherlands uses mixed-type antennas and receivers. The experimental data was collected from 13th to 15th, Oct. 2012 with an

Table 39.1 Antenna and receiver type of receivers used for experiment

Networks	Station name	Antenna type	Receiver type	Role in validation
China	ROV1	TRM59800.00	TRIMBLE NETR8	Rover
	REF1	TRM59800.00	TRIMBLE NETR8	40 km inter-station distance of network
	REF2	TRM59800.00	TRIMBLE NETR8	
	REF3	TRM59800.00	TRIMBLE NETR8	
	REF4	TRM59800.00	TRIMBLE NETR8	
	REF5	TRM59800.00	TRIMBLE NETR8	80 km inter-station distance of network
	REF6	TRM59800.00	TRIMBLE NETR8	
	REF7	TRM59800.00	TRIMBLE NETR8	
The Netherlands	LITH	S2SPG_A1+M	Topcon ODYSSEY_E	Rover
	CABA	ASH700936C_M	ASHTECH Z-XII3	40 km inter-station distance of network
	EHVN	S2SPG_A1+M	Topcon ODYSSEY_E	
	KOSG	AOAD/M_B	LEICA GRX1200GGPRO	
	BOXM	S2X3G+C+M	Topcon ODYSSEY_E	
	DELF	TRM29659.00	TRIMBLE 4700	80 km inter-station distance of network
	LELY	S2SPG_A1+M	Topcon ODYSSEY_E	
	ROE2	S2SCR.G3+M2	Topcon ODYSSEY_E	

interval of 30 s. The software of SF PPP is developed based on RTKLIB which is an open sources program package for GNSS Positioning (http://www.rtklib.com) [35, 36]. The experiment is carried out in a simulated real-time mode and the processing steps of ionospheric delay correction at each epoch are the following:

(1) Determine the LOS ionospheric TEC and its variance for each pair of satellite and reference receiver with dual-frequency PPP method [48]. The precise satellite orbit and clock from CODE, the satellite and receiver DCB estimated using IGGDCB is adopted in the determination of LOS ionospheric TEC. The IGGDCB is a two-step method for DCB determination, which can work well with only a few ground tracking stations [25]. In practice, the DCB product can be obtained in the previous day because DCB is relatively stable over days.

(2) Predict the LOS ionospheric delay for each pair of satellite and rover receiver based on the approach of LIM and SIM respectively. The variance of corresponding ionospheric delay is also estimated based on the law of error propagation. In this step, the GIM is also introduced to calculate the LOS ionospheric delay for rover based on the method described in Sect. 39.2.1.

(3) Positioning based on SF PPP with the ionospheric delay predicted by different approaches in step (2). The predicted ionospheric delay is considered as a pseudo-observation with an estimated variance in SF PPP for the mitigation. Only the code and phase on frequency L1 from rover receiver is used and the satellite orbit, satellite clock and DCB are corrected by the product from

CODE and IGGDCB. The elevation-dependent weight is applied to the raw observation and the cut-off elevation is 10^0. Although the rover is static, the positioning is processed in a dynamic mode with Kalman filter.

(4) Repeating steps (1)–(3), the rover data could be processed epoch by epoch.

39.3.2 Accuracy of Predicted Ionospheric Delay for Rover

The LOS ionospheric delay extracted from the dual-frequency data of rover receiver can be taken as 'true' ionospheric delay and used to validate the accuracy of predicted ionospheric delay from GIM, LIM and SIM. The root mean square (RMS) is used as a measure of accuracy, which is calculated as:

$$RMS_t = \sqrt{\frac{\sum_{i=1}^{S_t} \Delta_{i,t}^2}{S_t}} \tag{39.4}$$

where, RMS_t is the accuracy of predicted ionospheric delay at epoch t; $\Delta_{i,t}$ is the difference between predicted and 'true' ionospheric delay for satellite i; S_t is the total number of visible satellites with the cut-off elevation of $10°$.

The accuracy comparison between three ionospheric modeling methods is presented in Figs. 39.3 and 39.4. Figure 39.3 shows the RMS of predicted ionospheric delay in 40 km inter-station distance network and Fig. 39.4 shows the corresponding result in 80 km inter-station distance network. It can be seen that the ionospheric delay prediction using GIM has a lower accuracy in China area (RMS < 3 m) than in the Netherlands (RMS < 1 m).

Results in Figs. 39.3 and 39.4 also show that the accuracy of ionospheric delay prediction using SIM is much better than that of LIM and GIM in both China and the Netherlands. The accuracies of GIM and LIM in local afternoon (about 11:00–16:00, UTC) are much worse than that in other period, whereas the accuracy of SIM is basically the same during whole day. The reason is that the ionospheric activities usually reach a relatively high level in the afternoon and the variations in ionospheric delay may become more complex, and are difficult to be captured by GIM and LIM. Moreover, the error of ionospheric thin-layer assumption and mapping function will also become larger with high ionospheric activities. Unlike with GIM and LIM, the SIM has the ability of capturing this complex variations in ionospheric delay and can predict the ionospheric delay with more accuracy. It should be pointed out that GIM in China (about 1.0–2.0 m) has much poorer accuracy than in the Netherlands (about 0.40–0.80 m). It is because only 4–6 monitoring stations in China are contributed to IGS GIM generation, while more than 50 stations in Europe are used.

The mean and standard deviation of SIM, LIM and GIM accuracies during the experimental period are shown in Table 39.2. The mean accuracy of SIM and LIM
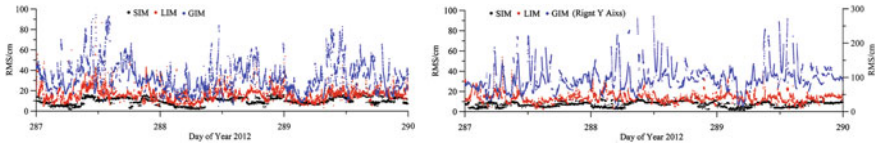
Fig. 39.3 Accuracy of ionospheric delay predicted using different approaches with an inter-station distance of 40 km in the Netherlands (*left*) and China (*right*)
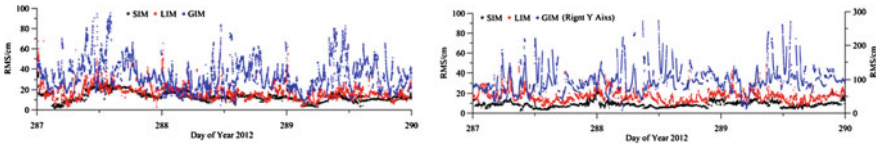
Fig. 39.4 Accuracy of ionospheric delay predicted using different approaches with an inter-station distance of 80 km in the Netherlands (*left*) and China (*right*)

Table 39.2 Mean and standard deviation of the accuracies of SIM/LIM/GIM in China and the Netherlands

| Networks	SIM/cm		LIM/cm		GIM/cm
	40 km	80 km	40 km	80 km	
China	7.1 ± 2.1	8.9 ± 2.2	13.8 ± 5.6	16.3 ± 4.9	96.0 ± 34.5
The Netherlands	9.9 ± 2.8	12.5 ± 4.7	15.4 ± 6.0	17.0 ± 7.4	33.8 ± 14.0

in China is about 2–3 cm better than that in the Netherlands. This may be because the network in China is equipped with identical receivers and antennas at each station while the network in the Netherlands uses a variety of receivers and antennas. Overall, the ionospheric delay predicted by SIM achieves better than 10 cm accuracy in 40 km inter-station network and about 13 cm accuracy in 80 km inter-station network. The accuracy of LIM, which is about 15 cm (40 km) and 17 cm (80 km), is a bit lower than SIM. The GIM is not as good as the other two methods and it only achieves about 0.4 and 1.0 m accuracy level in the Netherlands and China respectively.

39.3.3 Positioning Accuracy of SF PPP

The ionospheric delay predicted with three different methods is applied to SF PPP and the positioning results are compared in this section. The dual-frequency PPP results in static mode are used as 'true' rover position. The SF PPP results based on GIM, LIM and SIM are presented in Figs. 39.5, 39.6, 39.7. The accuracy is illustrated on the eastern, northern and up components in local coordinate system.
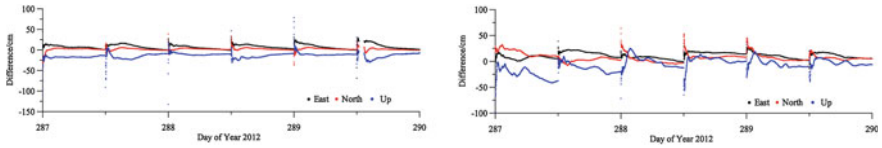
Fig. 39.5 Positioning result of SF PPP based on SIM (*left*) and LIM (*right*) with 40 km reference stations in the Netherlands
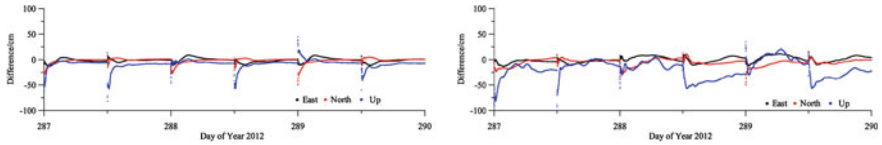
Fig. 39.6 Positioning result of SF PPP based on SIM (*left*) and LIM (*right*) with 40 km reference stations in China
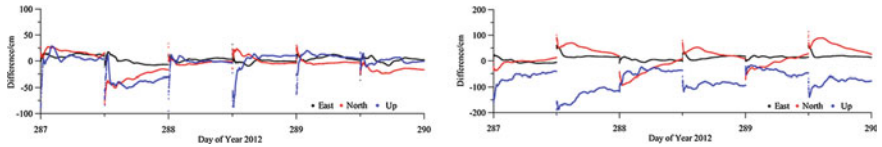
Fig. 39.7 Positioning result of SF PPP based on GIM in the Netherlands (*left*) and China (*right*) respectively

The Kalman filter in SF PPP is reset every 12 h to investigate the convergence time. Due to the limitation of space, the results based on 80 km reference stations are absent here.

It is shown by the positioning results that the initial positioning accuracy of SF PPP in each session based on SIM and LIM is almost the same (about 0.25 m), but the positioning accuracy based on SIM converges much better than that based on LIM with the data accumulation, particularly in the up component. The reason may be that the predicted ionospheric delay based on LIM is less accurate during ionospheric activity as shown by Figs. 39.3 and 39.4. The accuracy of GIM-based SF PPP can be improved significantly with the data accumulation in the Netherlands, while the improvement is not so significant in China and a systematic bias also exists in the up component. The positioning accuracy of SF PPP based on GIM in the Netherlands is much better than that in China. This result further indicates that the GIM is not very suitable for SF PPP user in China.

The average positioning accuracies of SF PPP in eastern, northern and up components in the Netherlands and China are summarized in Tables 39.3 and 39.4 respectively. The first 1 h in each session is considered as the convergence process and artificially excluded in the statistic. Compared with LIM, the SIM can improve the positioning accuracy about 20 %, especially in China area. The positioning

Table 39.3 Average positioning accuracy of SF PPP based on SIM, LIM and GIM in the Netherlands

Models		E/cm			N/cm			U/cm		
		Mean	STD	RMS	Mean	STD	RMS	Mean	STD	RMS
40 km	SIM	7.1	4.9	8.7	2.1	1.8	2.7	−13.2	4.3	13.9
	LIM	10.9	5.6	12.3	6.5	6.5	9.2	−7.0	12.7	14.5
80 km	SIM	4.7	3.9	6.1	1.9	1.6	2.5	−13.9	4.8	14.7
	LIM	7.0	5.4	8.8	3.9	5.5	6.8	−4.7	17.8	18.4
	GIM	2.8	5.9	6.6	−6.1	15.8	16.9	−2.9	18.1	18.3

Table 39.4 Average positioning accuracy of SF PPP based on SIM, LIM and GIM in China

Models		E/cm			N/cm			U/cm		
		Mean	STD	RMS	Mean	STD	RMS	Mean	STD	RMS
40 km	SIM	−1.0	3.8	3.9	−0.6	2.3	2.3	−7.0	3.4	7.7
	LIM	0.0	5.9	5.9	−4.7	5.5	7.3	−17.1	16.5	23.7
80 km	SIM	−1.7	4.7	5.0	−0.2	3.1	3.1	−6.8	5.1	8.5
	LIM	2.6	5.9	6.5	−3.9	6.9	7.9	−8.3	15.6	17.7
	GIM	9.8	8.9	13.3	15.8	36.3	39.6	−71.8	33.5	79.2

accuracy (RMS) of SF PPP in the Netherlands based on SIM is about 0.06–0.10 m and 0.13–0.15 cm in the horizontal and vertical components respectively and it is about 0.04–0.06 m and 0.07–0.09 m in China.

Applying GIM, the positioning accuracy of SF PPP is about 0.18 m in the Netherlands, whereas it is only about 0.40 m (horizontal) and 0.8 m (vertical) in China. The positioning result of SF PPP in China can hardly reach a sub-meter accuracy level with GIM ionospheric delay correction. Therefore, it is necessary to introduce some reference stations in China to provide more accurate ionospheric delay for SF PPP of sub-meter accuracy level.

In addition, comparing to the 'true' position, there is a systematic bias on the up component in all three methods. This bias may result from the residual error of ionospheric delay after applying the corrections, but it is still not confirmed so far.

39.3.4 Convergence Time of SF PPP

In addition to positioning accuracy, the convergence time is also very important for the real-time application of SF PPP. It is defined as the time to reach required accuracy level and the accuracy can be kept for at least 2 h in this experiment. The accuracy of 1.0, 0.75, 0.50 and 0.25 m in horizontal and vertical components is selected for the convergence time statistics respectively. Tables 39.5 and 39.6 show the convergence time of SF PPP based on LIM, SIM and GIM in the Netherlands and China respectively. The number shown in Tables 39.5 and 39.6 is

Table 39.5 Convergence time of SF PPP based on SIM, LIM and GIM in the Netherlands (*unit* epoch number with a measurement interval of 30s)

Distances of inter-station	Models		Accuracy			
			<100 cm	<75 cm	<50 cm	<25 cm
40 km	SIM	Horizontal	1.0	1.0	1.2	14.2
		Vertical	1.2	1.8	2.7	10.5
	LIM	Horizontal	1.0	1.0	4.3	15.9
		Vertical	1.2	1.7	7.8	28.8
80 km	SIM	Horizontal	1.0	1.0	1.0	14.5
		Vertical	1.0	1.5	2.3	18.2
	LIM	Horizontal	1.0	1.0	3.0	16.1
		Vertical	1.7	3.2	14.3	28.4
	GIM	Horizontal	1.0	2.0	7.0	19.6
		Vertical	1.7	10.3	22.8	39.2

Table 39.6 Convergence time of SF PPP based on SIM, LIM and GIM in China (*unit* epoch number)

Distances of inter-station	Models		Accuracy			
			<100 cm	<75 cm	<50 cm	<25 cm
40 km	SIM	Horizontal	1.0	1.0	1.5	23.5
		Vertical	1.0	1.2	19.2	58.3
	LIM	Horizontal	1.0	1.0	1.7	23.5
		Vertical	1.2	9.7	50.8	130.7
80 km	SIM	Horizontal	1.0	1.0	1.7	34.0
		Vertical	1.0	1.5	17.7	59.0
	LIM	Horizontal	1.0	1.0	2.0	38.5
		Vertical	1.2	2.2	56.2	114.5
	GIM	Horizontal	3.0	67.3	–	–
		Vertical	57.0	–	–	–

Note '–' means the corresponding accuracy is impossible to be achieved

the average epoch number for the convergence of all the six sessions. If the convergence time is longer than 2 h, the convergence time is regarded as infinite or accuracy requirement is not achievable.

The convergence time of SF PPP based on GIM becomes longer and longer when the required accuracy is better than 0.5 m on horizontal and vertical components and the SF PPP based on GIM even doesn't converge to the accuracy better than 0.75 m in China shown in Table 39.6. The results also show that the convergence time of SF PPP based on LIM and SIM is much shorter than that based on GIM. With the convergence time of about 1.5 min, the positioning accuracy of SF PPP based on SIM is better than 0.5 m in the Netherlands and better than 0.5 m (horizontal)/0.75 m (vertical) in China respectively. For the vertical accuracy of 0.5 m, the convergence time of SF PPP based on SIM in the Netherlands is only about 2 min, while that based on LIM is more than 4–7 min.

The convergence time of SF PPP based on LIM is about twice longer than that of SIM in term of the vertical accuracy. The superiority of SIM is more significant when a high level of accuracy is required, e.g. 0.5 or 0.25 m.

Therefore, it is further demonstrated that IGS released GIM is not feasible for sub-meter level SF PPP requirement in China. In the approach of ionospheric modeling, the error from the ionospheric thin-layer assumption and the mapping function may indeed not be ignorable and it may slow down the convergence of SF PPP very significantly, particularly in the vertical component.

39.3.5 Suggestions and Recommendations

It is feasible to use the SF PPP technique for achieving sub-meter positioning in real-time or near real-time mode. The IGS released GIM is able to aid the SF PPP achieving a positioning with 0.4–0.6 m accuracy based on 10–20 min accumulation observation in the Netherlands, whereas it is currently nearly invalid for the sub-meter SF PPP user in China. Additionally, the results also show that more Chinese stations should be considered in the GIM computation.

The performance of LIM is almost the same as that of SIM for SF PPP users requiring 0.75 m accuracy, but SIM is much better than LIM for the SF PPP users requiring 0.5 m accuracy. SF PPP based on LIM can achieve positioning accuracy better than 0.5 m with 1–2 min accumulation data. The results also indicate that the error resulting from ionospheric thin-layer and mapping function cannot be ignored directly for the precise ionospheric delay correction.

Therefore, a reference station network with 40–80 km inter-station distance is suggested to be set up for SF PPP user requiring sub-meter accuracy level in China and it can also be considered as an alternative for GIM in the Netherlands for the high precise SF PPP. SIM is recommended to be used for predicting the ionospheric delay correction at the rover rather than LIM. Based on SIM, the ionospheric delay is modeled on a satellite basis and independent of the ionospheric thin-layer assumption and mapping function.

39.4 Application of SIM in GPS/BDS Data

The Chinese BeiDou Navigation Satellite System (BDS) began to provide positioning, navigation and timing services (PNT) in the Asia-Pacific areas from the end of December, 2012 [2]. Currently, nearly 20 GPS and BDS satellites can be tracked in the Asia-Pacific region and the data of GPS and BDS can be combined together for SF PPP user. In this section, SIM, the recommend approach for ionospheric delay correction in Sect. 39.3, will be applied to SF PPP using GPS and BDS data and the positioning accuracy and convergence time will be analyzed.

Fig. 39.8 Distribution of
experimental GPS+BDS
receivers located in Beijing,
China
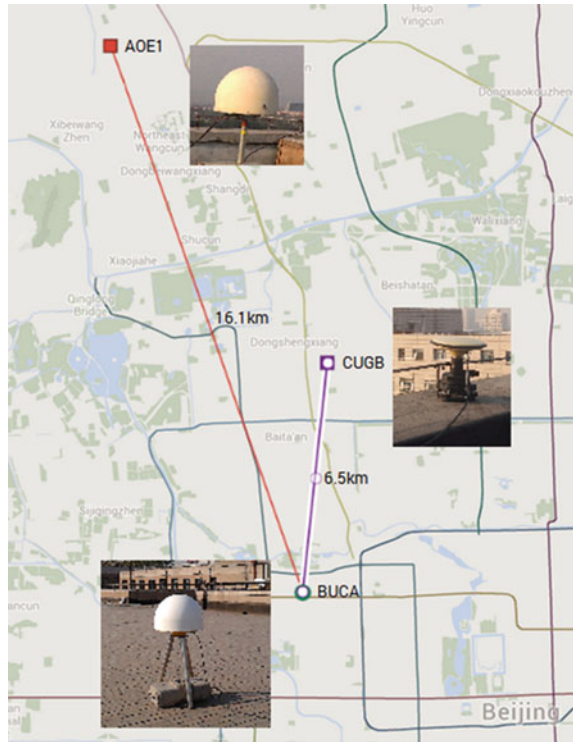
39.4.1 Description of GPS and BDS Data

Three GPS/BDS receivers were used to collect GPS and BDS data in Beijing, China
on 13th Nov., 2013 for this experiment. These receivers are located in Academy of
Opto-Electronics belonging to Chinese Academy of Sciences, China University of
Geosciences (Beijing), and Beijing University of Civil Engineering and Architec-
ture and named as AOE1, CUGB and BUCA respectively. Figure 39.8 shows the
distribution of these stations and installed antennas. The types of antenna and
receiver at AOE1 and BUCA are CC40GE and N71 M produced by CHC (http://
www.chcnav.com/), whereas those at CUGB are GPS 704X and UR240-CORS-II
produced by UNICORE (http://www.unicorecomm.com/).

In this experiment, BUCA receiver is selected as the rover station and the other
two receivers (AOE1 and CUGB) are selected as reference stations. The length of
baseline AOE1-BUCA is about 16.1 km and it is about 6.5 km for baseline
CUGB-BUCA. Due to the limited number of contributed receivers, it is difficult to
form a network with different inter-station distances. Thus, AOE1 and CUGB are
individually considered as reference stations to provide the ionospheric delay
correction for rover BUCA, so that the performance of SIM can be assessed with
different inter-station distances.
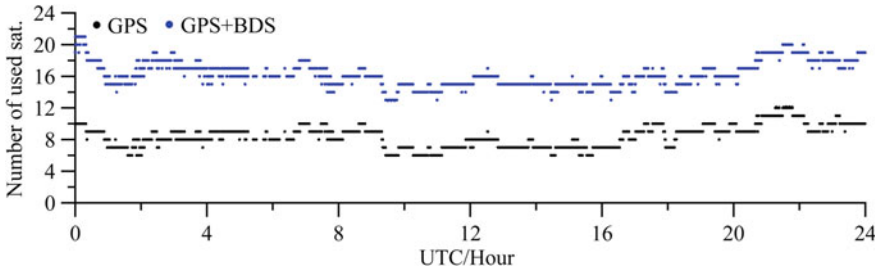
Fig. 39.9 Number of GPS and BDS satellites tracked by rover BUCA with the cut-off elevation of 10°

Currently, there are in total 14 BDS satellites in orbit consisting of five GEO satellites at the altitude of 35,786 km, five IGSO satellites at the altitude of 35,786 km with 55° inclination and four MEO satellites at the altitude of 21,528 km with 55° inclination [2]. Figure 39.9 illustrates the number of GPS and GPS + BDS satellites tracked by BUCA receiver at each epoch with the cut-off elevation of 10°. It can be seen that 7–9 GPS and 8–12 BDS satellites are observed during the whole day respectively.

The steps of data processing are the same as that described in Sect. 39.3.1, but it should be pointed out that (1) the DCB in GPS satellite is corrected using the CODE-released product and the DCB in BDS satellite and three receivers are estimated using IGGDCB; (2) the biases of receiver/satellite antenna phase center have not been calibrated in our experiment.

39.4.2 Result of GPS and GPS+BDS SF PPP

The accuracy of predicted ionospheric delay and positioning result of SF PPP based on a preliminary GPS/BDS dataset will be explored in this section, as well as the convergence time of SF PPP. Since there is only one reference station (AOE1 or CUGB), the predicted ionospheric delay at rover is actually the corresponding value obtained from each reference receiver. Assuming the ionospheric delay extracted from the dual-frequency observation of rover is true value, the mean and standard deviation of the accuracy of GPS/BDS ionospheric delay predicted from different reference stations is shown in Table 39.7. The whole day is divided into six periods with four-hour interval. It can be seen that the accuracies of ionospheric delay predicted from GPS and BDS satellites are almost the same. According to the daily characteristic of ionospheric activity, the accuracy becomes a little poorer in local afternoon (08:00:00–12:00:00, UTC). The result also shows that the accuracy of ionospheric delay predicted from AOE1 is better than that from CUGB, although the distance from rover to CUGB is much shorter than that from rover to AOE1. The reason may be that the receiver and antenna specific

Table 39.7 Mean and standard deviation of the accuracies of GPS/BDS ionospheric delay

Sessions	SIM-AOE1/cm		SIM-CUGB/cm	
	GPS[a]	BDS[a]	GPS[a]	BDS[a]
00:00:00–04:00:00	12.1 ± 7.0	16.5 ± 4.9	20.5 ± 6.6	20.1 ± 3.6
04:00:00–08:00:00	17.9 ± 6.5	15.3 ± 5.2	28.5 ± 4.3	31.0 ± 6.0
08:00:00–12:00:00	21.4 ± 7.8	9.7 ± 4.2	24.2 ± 3.8	27.7 ± 4.3
12:00:00–16:00:00	18.4 ± 4.4	11.7 ± 3.5	20.3 ± 5.1	21.8 ± 3.6
16:00:00–20:00:00	17.2 ± 6.6	16.7 ± 1.7	28.2 ± 9.0	24.7 ± 1.9
20:00:00–24:00:00	13.3 ± 5.1	16.4 ± 6.3	21.2 ± 6.3	26.5 ± 6.1
Mean	15.6 ± 5.5		24.6 ± 5.4	

[a] Number before "±" is the mean and that after "±" is the corresponding standard deviation
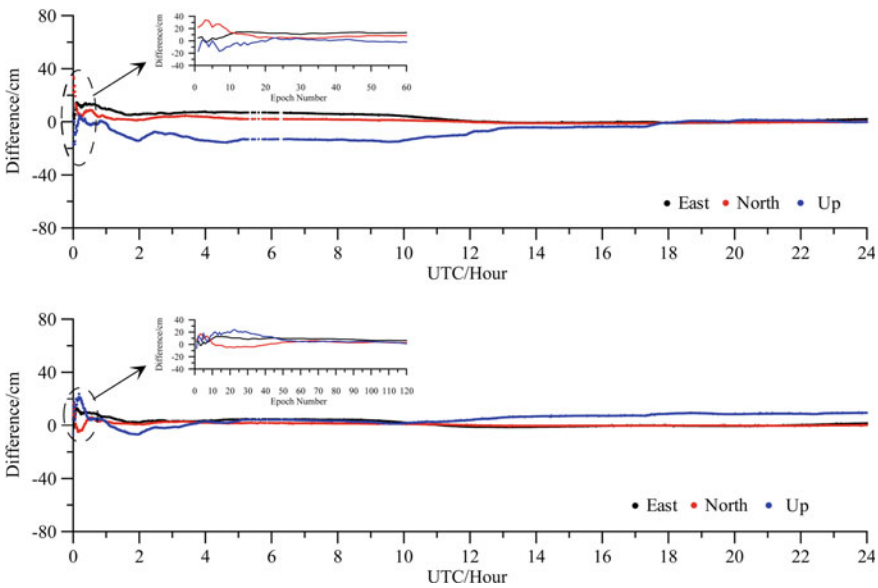
Fig. 39.10 Positioning results of SF PPP using the ionospheric delay predicted from AOE1 based on GPS (*upper*) and GPS+BDS (*lower*) respectively

biases can be completely eliminated in this case. Overall, the ionospheric delay predicted from AOE1 reach the accuracy level of about 0.16 m, while that from CUGB is about 0.25 m. This accuracy is comparable with that demonstrated by GPS data in Sect. 39.3.2.

Figure 39.10 shows the differences between estimated and 'true' coordinates of rover in eastern, northern and up components using the predicted ionospheric delay from AOE1 (inter-station distance of about 16.1 km). The upper panel shows the positioning result with GPS data, while the lower panel shows the positioning result using GPS + BDS data. The 'true' position of rover is calculated with dual-frequency PPP technique using GPS only data. Figure 39.11 shows
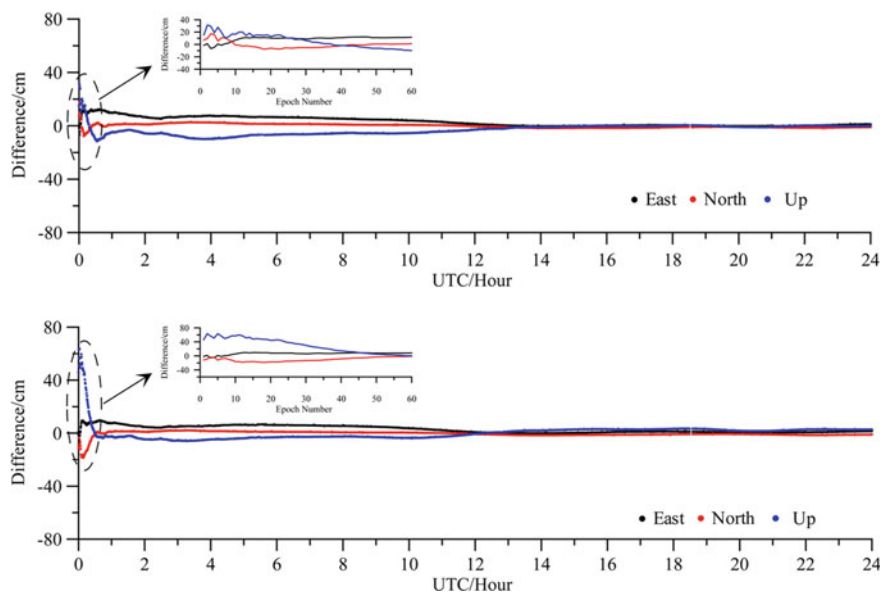
Fig. 39.11 Positioning results of SF PPP using the ionospheric delay predicted from CUGB based on GPS (*upper*) and GPS+BDS (*lower*) respectively

Table 39.8 Daily positioning accuracy of GPS/BDS SF PPP based on the ionospheric delay predicted from AOE1 and CUGB

Accuracy	SIM-AOE1/cm		SIM-CUGB/cm	
	GPS	GPS + BDS	GPS	GPS + BDS
Horizontal	4.2	2.6	4.2	3.7
Vertical	5.7	4.3	4.6	3.1

the similar positioning result based on the reference station of CUGB (inter-station distance of about 6.5 km).

Except the results shown by the lower panel of Fig. 39.11, the positioning accuracy SF PPP in eastern, northern and up components at the first epoch is better than 0.5 m when applying the ionospheric delay correction based on SIM. Compared with the positioning result based on GPS alone, the combination of GPS data BDS data could improve the instantaneous positioning accuracy of SF PPP (lower panel of Fig. 39.10 but not 39.11). This high accurate instantaneous positioning is advantageous to reduce the convergence time of SF SPP.

The positioning accuracy of SF PPP using 24-h data is given by Table 39.8. It can be seen that the horizontal and vertical accuracy of SF PPP is better than 0.05 and 0.06 m respectively. The accuracy of SF PPP with SIM ionospheric delay correction is comparable with dual-frequency PPP without ambiguity fixing.

Table 39.9 Convergence time of SF PPP based on reference station AOE1 and CUGB using GPS/BDS data (*unit* epoch number)

		50–100 cm		25–50 cm		<25 cm	
		GPS	GPS + BDS	GPS	GPS + BDS	GPS	GPS + BDS
AOE1	Horizontal	1	1	1	1	8	1
	Vertical	1	1	1	1	1	1
CUGB	Horizontal	1	1	1	1	1	1
	Vertical	1	1	1	15	6	33

The convergence time for different positioning accuracies is summarized in Table 39.9. In order to see the convergence process clearly, the positioning results during the first 2 h in Figs. 39.10 and 39.11 are also zoomed in. It can be seen that the positioning with 0.25 m horizonal accuracy can be achieved by single epoch SF PPP based on the ionospheric delay correction using SIM. In term of the result based on reference station AOE1, the convergence time can be reduced significantly when a more accurate positioning is required (e.g. better than 0.25 m). However, the result based on reference station CUGB shows that the convergence time for vertical component become longer when combining GPS and BDS data. The reason needs to be further analyzed.

Based on the here presented analysis, it suggests that SIM approach can provide the ionospheric delay at the accuracy level of 0.2 m and improve single epoch SF SPP to reach the sub-meter positioning accuracy level using GPS and BDS data. The accuracy of SF PPP result based on ionospheric delay correction from SIM in one day is about 0.05 and 0.06 m in horizontal and vertical components respectively. In order to obtain a much better ionospheric delay correction, the same antenna and receiver is suggested to be used in the reference and rover station. Experiment result also suggests that the combined GPS and BDS data can further improve the vertical accuracy of SF PPP and reduce the convergence time.

39.5 Conclusions and Future Works

The PPP technique with single frequency receiver is one of the potential approaches to achieve a sub-meter (better than 0.5 m) positioning with low cost. The ionospheric delay, as the toughest error sources in SF PPP, has to be mitigated as much as possible to realize this goal. This paper has reviewed the commonly used ionospheric delay mitigation method for single frequency user, including global ionospheric map released by IGS, local ionospheric model based on second-order polynomial and satellite based ionospheric delay model. The performances of different approaches are assessed and compared using two GPS networks from China and the Netherlands with different inter-station distances. The assessment is carried out in the following three aspects: accuracy of predicted ionospheric delay, positioning accuracy and convergence time of SF PPP.

Comparison result demonstrates that: (1) the IGS released GIM can currently not aid SF PPP achieving a positioning with sub-meter accuracy in China, whereas it is effective for SF PPP users of sub-meter accuracy level in the Netherlands; (2) A reference network surrounding the rover with 40–80 km is necessary for SF PPP in China to meet the sub-meter positioning requirement; (3) A satellite based ionospheric model (SIM) in which the ionospheric thin-layer assumption and mapping function can be avoided is suggested for SF PPP based on a regional reference network rather than the traditional ionospheric modeling method.

Following these suggestions and recommendations, the SIM has been applied to SF PPP based on a limited GPS and BDS dataset gathered in Beijing, China. Numerical result demonstrates that the SF PPP based on SIM can achieve a sub-meter positioning accuracy, even with single epoch. Compared with the result only based on GPS data, the combined GPS and BDS data can improve the accuracy about 20 % and reduce the convergence time, particularly in the vertical component.

However, the period of experimental data collection and distribution of receiver location are all at a medium level of ionospheric activities, the drawn conclusions may be more conservative for low ionospheric activities as well as being relatively short and optimistic for high ionospheric activities; thus, more experiment should be further carried out in different levels of ionospheric activates. In addition, the inconsistency of different types of antenna and receiver between rover and reference stations needs to be further analyzed.

References

1. Allain D, Mitchell C (2009) Ionospheric delay corrections for single-frequency GPS receivers over Europe using tomographic mapping. GPS Solut 13(2):141–151
2. BD-SIS-ICD (2012) BeiDou navigation satellite system signal in space interface control document, China Satellite Navigation Office, Beijing
3. Bisnath S, Gao Y (2008) Current state of precise point positioning and future prospects and limitations. In: Sideris MG (ed) Observing our changing earth, vol 133, pp 615–623

4. Bree RP, Tiberius CJM (2012) Real-time single-frequency precise point positioning: accuracy assessment. GPS Solut 16(2):259–266
5. Chen K, Gao Y (2005) Real-time precise point positioning using single frequency data. Paper presented at proceedings of ION GNSS 2005, Long Beach, CA
6. Coco DS et al (1991) Variability of GPS satellite differential group delay biases. IEEE Trans Aerosp Electron Syst 27(6):931–938
7. Conte J et al (2011) Accuracy assessment of the GPS-TEC calibration constants by means of a simulation technique. J Geodesy 85(10):707–714
8. Feess WA, Stephens SG (1987) Evaluation of GPS ionospheric time-delay model. IEEE Trans Aerosp Electron Syst AES-23(3):332–338
9. Feltens J et al (1998) Routine production of ionosphere TEC maps at ESOC-first results (IGS presentation). Paper presented at proceedings of the 1998 IGS AC workshop, ESOC, Darmstadt, Germany
10. Feltens J (2007) Development of a new three-dimensional mathematical ionosphere model at European Space Agency/European Space Operations Centre. Space Weather 5(S12002):1–17
11. Geng J et al (2010) Rapid re-convergences to ambiguity-fixed solutions in precise point positioning. J Geodesy 84(12):705–714
12. Georgiadiou Y (1994) Modeling the ionosphere for an active control network of GPS stations. LGR-Series-Publications of the Delft Geodetic Computing Centre, vol 7
13. Hernández-Pajares M et al (1999) New approaches in global ionospheric determination using ground GPS data. J Atmos Solar Terr Phys 61(16):1237–1247
14. Hernández-Pajares M (2004) IGS ionosphere WG status report: performance of IGS ionosphere TEC maps (Position paper)
15. Hernández-Pajares M (2006) Summary and current status of IGS ionosphere WG activities—a potential future product: global maps of effective ionospheric height. In: IGS technical workshop
16. Hernández-Pajares M et al (2009) The IGS VTEC maps: a reliable source of ionospheric information since 1998. J Geodesy 83(3):263–275
17. IS-GPS (2004) Navstar GPS space segment/navigation user interfaces (ICD-GPS-200D), Revision D. ARINC Engineering Services, LLC, El Segundo, CA
18. Klobuchar JA (1987) Ionospheric time-delay algorithm for single-frequency GPS users. IEEE Trans Aerosp Electron Syst AES-23(3):325–331
19. Komjathy A et al (2005) Automated daily processing of more than 1000 ground-based GPS receivers for studying intense ionospheric storms. Radio Sci 40(6):S6006
20. Kouba J, Héroux P (2001) Precise point positioning using IGS orbit and clock products. GPS Solut 5(2):12–28
21. Kouba J (2009) A guide to using International GNSS Service (IGS) products. http://www.igs.org/igscb/resource/pubs/UsingIGSProductsVer21.pdf
22. Lanyi G et al (1988) A comparison of mapped and measured total ionospheric electron content using global positioning system and beacon satellite observations. Radio Sci 23(4):483–492
23. Le AQ et al (2008) Use of global and regional ionosphere maps for single-frequency precise point positioning. In: Sideris MG (ed) Observing our changing Earth international association of Geodesy symposia
24. Li X et al (2013) A method for improving uncalibrated phase delay estimation and ambiguity-fixing in real-time precise point positioning. J Geodesy 87(5):405–416
25. Li Z et al (2012) Two-step method for the determination of the differential code biases of COMPASS satellites. J Geodesy 86(11):1059–1076
26. Liu J et al (2010) Spherical cap harmonic model for mapping and predicting regional TEC. GPS Solut 15(2):109–119
27. Mannucci AJ et al (1999) GPS and ionosphere: review of radio science 1996–1999. Oxford University Press, New York
28. Odijk D et al (2014) Single-frequency PPP-RTK: theory and experimental results. In: Proceedings of the IAG general assembly, Melbourne, Australia, pp 571–578

29. Orús R et al (2002) Performance of different TEC models to provide GPS ionospheric corrections. J Atmos Solar Terr Phys 64(18):2055–2062
30. Orús R et al (2005) Improvement of global ionospheric VTEC maps by using kriging interpolation technique. J Atmos Solar Terr Phys 67(16):1598–1609
31. Schaer S et al (1998) IONEX: the IONosphere map EXchange format version 1. Paper presented at proceedings of the IGS AC Workshop, Darmstadt, Germany
32. Schaer S (1999) Mapping and predicting the earth's ionosphere using the global positioning system. Ph D thesis, Astronomical Institutes, University of Bern, Berne, Switzerland
33. Schüler T et al (2011) Precise ionosphere-free single-frequency GNSS positioning. GPS Solut 15(2):139–147
34. Shi C et al (2012) An improved approach to model ionospheric delays for single-frequency precise point positioning. Adv Space Res 49(12):1698–1708
35. Takasu T, Yasuda A (2009) Development of the low-cost RTK-GPS receiver with an open source program package RTKLIB. In: International symposium on GPS/GNSS, International Convention Center Jeju, Korea November 4–6
36. Takasu T (2009) RTKLIB: open source program package for RTK-GPS. In: FOSS4G 2009, Tokyo, Japan
37. Tiberius C et al (2011) Staying in lane: real-time single-frequency PPP on the road. In: Proceedings of inside GNSS(November/December), pp 48–53
38. Wu X et al (2012) Evaluation of COMPASS ionospheric model in GNSS positioning. Adv Space Res 51(6):959–968
39. Yuan Y, Ou J (2004) A generalized trigonometric series function model for determining ionospheric delay. Prog Nat Sci 14(11):1010–1014
40. Yuan Y et al (2008) Refining the Klobuchar ionospheric coefficients based on GPS observations. IEEE Trans Aerosp Electron Syst 44(4):1498–1510
41. Zhang B (2013) Study on the theoretical methodology and applications of precise point positioning using un-differenced and uncombined GNSS data. Graduate University of Chinese Academy of Sciences, Wuhan, China
42. Zhang H et al (2013) On the convergence of ionospheric constrained precise point positioning based on undifferential uncombined raw observation. Sensors 13:15708–15725
43. Zou X et al (2012) A new ambiguity resolution method for PPP using CORS network and its real-time realization. Paper presented at China Satellite Navigation Conference (CSNC) 2012. Springer, Berlin/Heidelberg, Germany, Guangzhou, China
44. Zumberge JF et al (1997) Precise point positioning for the efficient and robust analysis of GPS data from large networks. J Geophys Res Solid Earth 102(B3):5005–5017
45. Ding W (2012) Research on key technologies of real time precise point positioning system. Ph D thesis, University of Chinese Academy of Sciences, Wuhan, China (in Chinese)
46. Li Z (2012) Study on the mitigation of ionospheric delay and the monitoring of global ionospheric TEC based on GNSS/Compass. Ph D thesis, Institute of Geodesy and Geophysics, University of Chinese Academy of Sciences, Wuhan, China (in Chinese)
47. Wen J et al (2010) Experimental observation and statistical analysis of the vertical TEC mapping function. Chin J Geophys 53(1):22–29 (in Chinese)
48. Zhang B et al (2011) Determination of ionospheric observables with precise point positioning. Chin J Geophys 54(4):950–957 (in Chinese)